

# Identification of sleep and circadian alternative polyadenylation sites associated with APA-linked human brain disorders

**Carlos C. Flores**

Washington State University Spokane

**Nickolas A. Pasetto**

Washington State University Spokane

**Hongyang Wang**

Shanghai Academy of Agricultural Sciences

**Alexander Dimitrov**

Washington State University Vancouver

**Jon F. Davis**

Washington State University

**Zhuhua Jiang**

Washington State University

**Christopher J. Davis**

Washington State University Spokane

**Jason R. Gerstner** (✉ [j.gerstner@wsu.edu](mailto:j.gerstner@wsu.edu))

Washington State University Spokane

---

## Article

### Keywords:

**Posted Date:** January 18th, 2024

**DOI:** <https://doi.org/10.21203/rs.3.rs-3867797/v1>

**License:**   This work is licensed under a Creative Commons Attribution 4.0 International License.

[Read Full License](#)

**Additional Declarations:** Competing interest reported. J.G. is the founder of Blood Brain Biotechnology, LLC. All other authors declare no competing interests.

---

# Abstract

Sleep and circadian rhythm disruptions are comorbid features of many pathologies and can negatively influence numerous health conditions, including degenerative diseases, metabolic illnesses, cancer, and various neurological disorders. Genetic association studies linking sleep and circadian disturbances with disease susceptibility have mainly focused on changes in gene expression due to mutations, such as single-nucleotide polymorphisms. Thus, associations between sleep and/or circadian rhythm and alternative polyadenylation (APA), particularly in the context of other health challenges, are largely undescribed. APA is a process that generates various transcript isoforms from the same gene, resulting in effects on mRNA translation, stability, localization, and subsequent function. Here, we have identified unique APAs in rat brain that exhibit time-of-day-dependent oscillations in expression as well as APAs that are altered by sleep deprivation and the subsequent recovery period. Genes affected by APA usage include *Mapt/Tau*, *Ntrk2*, *Homer1A*, *Sin3band* and *Sorl*. *Sorl1* has two APAs which cycle with a 24 h period, one additional APA cycles with a 12 h period and one more that is reduced during recovery sleep. Finally, we compared sleep- or circadian-associated APAs with recently described APA-linked brain disorder susceptibility genes and found 46 genes in common.

## INTRODUCTION

Dysregulation of sleep and circadian rhythms can profoundly impact human health and compound disease<sup>1,2</sup>. Indeed, sleep disruption is associated with negative outcomes in cardiovascular, metabolic, immunologic, and cognitive health that can have substantial short- and long-term consequences<sup>3</sup>. Alterations in sleep and circadian rhythms are often observed with various brain disorders, including autism spectrum disorder, bipolar disorder, major depression, schizophrenia, Parkinson's, and Alzheimer's diseases<sup>4-7</sup>. Complicating the association between sleep and health is the fact that functional aspects of sleep remain largely undefined and inconclusive<sup>8,9</sup>; however, the use of evolutionarily distinct animal models to study sleep has historically offered keen insights<sup>10,11</sup>. For example, studies on circadian- and sleep-dependent gene-regulatory mechanisms in diverse species, including flies, rodents, and humans, have identified important phylogenetically conserved pathways with functional relevance<sup>12-14</sup>. Employing unbiased approaches, such as large-scale metabolomic, transcriptomic, and proteomic analyses, have also greatly aided in the generation of conceptual frameworks for characterizing sleep function in health<sup>14,15</sup>. Therefore, performing such discovery-based studies of sleep and circadian regulatory processes in model organisms will help define the fundamental biological mechanisms underlying sleep function and inform pre-clinical relevance for comorbidities of sleep dysfunction associated with poor health.

Alternative polyadenylation (APA) site usage is an important and often overlooked mechanism of gene regulation, that can affect mRNA stability, mRNA/protein targeting, translational competence, and generate alternative protein isoforms<sup>16,17</sup>. APA sites are common and occur most frequently in the 3' untranslated region (3' UTR) of mRNAs across phylogeny, with more than half of human genes having

multiple polyadenylation sites (PASs) that generate alternative isoforms<sup>18</sup>. These isoforms can have altered coding sequences or 3'UTRs, resulting in the diversification of cis-regulatory elements (e.g., RNA binding protein sites, microRNA binding sites) that influence transcript abundance, trafficking, stability, and/or translation efficiency<sup>19</sup>. Furthermore, there's growing evidence of cell-type-specific APA preference<sup>20</sup>. The involvement of APA in the context of sleep and circadian rhythms has been largely unexplored, with the few studies available mostly focused on peripheral organs<sup>21,22</sup> and cells<sup>23</sup>. Here, we have characterized how APA site usage oscillates based on the time of day as well as how it is altered following acute changes in sleep pressure, specifically in the adult mammalian brain. Multiple methodologies have been developed for transcriptome-wide profiling and mapping of APA sites<sup>24,25</sup>. To complete this study, we performed whole transcriptome termini sequencing (WTTS-seq)<sup>26,27</sup> analysis to profile the variations in APA usage that occur due to sleep pressure and daily rhythms in the rat forebrain. Over 31,000 PASs were recovered in total, with 45% of the represented genes having multiple APA sites. Interestingly, many of the PASs sequenced were not previously annotated in the rat genome. Moreover, a total of 2,011, (6%) of PASs cycled over the day, and 831 (3%) were homeostatically regulated following sleep loss following sleep loss or during recovery. Over half of all cycling or differentially expressed PASs were APAs, (i.e., in genes with  $\geq 2$  PASs). Given the importance of sleep<sup>4-7</sup> and APA in health and disease<sup>24,28,29</sup>, we compared our sequencing results with results from a recent study that determined APA usage in human brain disorder susceptibility<sup>30</sup>. The genes found in both studies warrant further examination and could lead to new rodent models to investigate these disorders.

To the best of our knowledge, the current study represents the first comprehensive, transcriptome-wide mapping of APA sites in adult mammalian brain tissue over the day-night cycle as well as following changes in sleep homeostasis. This global temporal dataset will be useful for future comparative studies that require the determination of baseline APA site usage profiles in the mammalian brain. Furthermore, our study underscores the importance of using alternative-omic approaches to characterize phylogenetically conserved genome-phenome information and reveals another expansive layer of complexity in sleep and circadian gene regulation that has not previously been documented.

## METHODS

**Subjects.** All animal procedures were carried out in accordance with the National Institutes of Health Guide for the Care and Use of Laboratory Animals and ARRIVE and OLAW guidelines and approved by the WSU Institutional Animal Care and Use Committee (IACUC; ASAF# 6804). Male Long Evans rats (7–9 weeks old) were housed in pairs at  $22 \pm 2^\circ\text{C}$  on a 12:12 h light-dark cycle. The rats were acclimated to this light cycle for at least 10 days prior to tissue collection, with water and chow *ad libitum*. Cages were cleaned weekly (between 8 and 11 AM) unless the rats were being euthanized within 24 h. Thirty rats were randomly assigned to one of six groups ( $n = 5/\text{group}$ ) that were sampled every 4 h, beginning 2 h after light onset (zeitgeber time (ZT)) (i.e., ZT2, 6, 10, 14, 18, and ZT22). For the sleep deprivation (SD) study, twenty rats were randomly assigned to 6 h SD from ZT0–6, wherein rats were kept awake by an automated bedding stir bar (Pinnacle) at the bottom of a cylindrical cage. The bar was set to rotate for 4

s, randomly changing rotation direction, and stopped for a random interval ranging from 10 to 30 s<sup>31,32</sup>. Following SD, rats ( $n = 5$ /time point) were euthanized immediately (R0) by live decapitation, or were returned to their home cage for 2 h (R2), 4 h (R4), or 8 h (R8) under red light without disruption before sampling. Five additional rats were euthanized at ZT8 as undisturbed, time-matched controls. The other time-matched controls with undisturbed sleep (i.e., ZT6, 10, and 14) were taken from the circadian analysis described above.

**Tissue Collection.** Rats were decapitated by guillotine under normal room light (ZT2–10) or under dim red light (ZT14–22). Following decapitation, forebrains were resected (Fig. 1A), frozen in 2-methylbutane suspended in dry ice, and then stored at  $-80^{\circ}\text{C}$  until homogenization for RNA extraction.

**RNA isolation.** Just before RNA isolation, forebrains were removed from  $-80^{\circ}\text{C}$  storage and placed on dry ice. Prior to use, a stainless-steel mortar and pestle were cleaned with RNase Zap (Thermo Fisher) and 70% ethanol. The mortar was then partially filled with liquid nitrogen before a forebrain was added, pulverized, and placed in a conical tube. Between each sample, the mortar and pestle were cleaned with 70% ethanol. A small aliquot of sample was removed for RNA isolation using Trizol Reagent (Invitrogen), according to the manufacturer's instructions. Purified RNA was resuspended in water, and concentration and purity were measured with a Nanodrop spectrophotometer (Thermo Fisher). Samples were stored at  $-20^{\circ}\text{C}$  until further processing was performed. WTTS-seq libraries were prepared as described by Zhou et al.<sup>26</sup>. Briefly, total RNA (2.5  $\mu\text{g}$ ) was incubated at  $70^{\circ}\text{C}$  with 10X Fragmentation buffer (Invitrogen) for 3 min. The fragmentation reaction was halted by the addition of Stop Solution and incubation on ice for at least 2 min. Next, poly(A) + RNA was purified from the fragmented total RNA with Dynabeads Oligo (dT)25 (Invitrogen), according to the manufacturer's directions, and used for first-strand cDNA synthesis in a 20  $\mu\text{L}$  reaction mixture. First, 1.0  $\mu\text{L}$  of barcode primer (100  $\mu\text{M}$ ) and 1.0  $\mu\text{L}$  of a common SMART primer (100  $\mu\text{M}$ ) were annealed to the poly(A) + RNA template by heating to  $65^{\circ}\text{C}$  for 5 min and incubating on ice for at least 2 min. Next, 4.0  $\mu\text{L}$  of 5X First-strand buffer (Invitrogen), 1.0  $\mu\text{L}$  of SuperScript III reverse transcriptase (Invitrogen), 1.0  $\mu\text{L}$  of 0.1 M dithiothreitol, 2.5  $\mu\text{L}$  of 10 mM dNTP, and 1.0  $\mu\text{L}$  of RNase OUT (Invitrogen) were added to the mixture. First-strand cDNA was synthesized by incubating the mixture at  $40^{\circ}\text{C}$  for 90 min in the presence of library-specific adaptors. Synthesis was terminated by heating the mixture at  $70^{\circ}\text{C}$  for 15 min. RNases I (100 U/ $\mu\text{L}$ ; Invitrogen) and H (2 U/ $\mu\text{L}$ ; Invitrogen) were subsequently added and incubated with the mixture at  $37^{\circ}\text{C}$  for 30 min to hydrolyze the remaining single-stranded RNA molecules and ensure that only single-stranded cDNA remained. RNase activities were terminated by heating the samples at  $70^{\circ}\text{C}$  for 20 min. Following purification with solid-phase reversible immobilization (SPRI) beads, second-strand cDNA was synthesized from first-strand cDNA by asymmetric PCR. In addition to the cDNA, the 50  $\mu\text{L}$  PCR reaction contained 1.0  $\mu\text{L}$  of Phusion Hi-Fidelity DNA polymerase, 10.0  $\mu\text{L}$  of 5X HF buffer, 1.0  $\mu\text{L}$  of 0.4  $\mu\text{M}$  barcode primer, 1.0  $\mu\text{L}$  of 0.8  $\mu\text{M}$  common primer, 1.0  $\mu\text{L}$  of 10 mM dNTP, and nuclease-free water. The PCR reaction was carried out by heating at  $95^{\circ}\text{C}$  for 30 sec, followed by 20 cycles of  $98^{\circ}\text{C}$  for 10 s,  $50^{\circ}\text{C}$  for 30 s, and  $72^{\circ}\text{C}$  for 30 s, with a final elongation step at  $72^{\circ}\text{C}$  for 10 min. SPRI beads were used to purify and select 200–500 bp

fragments from the final library. After quality control analyses, the size-selected library was sequenced with an Ion PGM Sequencer at the WSU Genomics Core Laboratory.

## Data analysis

**Raw read processing.** Raw data were obtained from 55 samples and stored in FASTQ format. We filtered raw reads with the FASTQ quality filter in the FASTX Toolkit (v0.0.13), allowing for a minimum score of  $\geq 10$  for  $\geq 50\%$  of bases ([http://hannonlab.cshl.edu/fastx\\_toolkit/](http://hannonlab.cshl.edu/fastx_toolkit/)). We trimmed T nucleotides or T-rich sequences located at the 5' ends of the reads using Perl scripts, as described in a previous study<sup>26</sup>. Trimmed reads of at least 16 bp in length were kept for further analysis.

**Read mapping and poly(A) site clustering.** For each data set, we aligned the processed reads to the *Rattus norvegicus* genome (mRatBN7.2/rn7) using the torrent mapping program (TMAP, v3.4.1; <http://github.com/iontorrent/tmap>) with the unique best hits parameter (-a 0). We then extracted raw PASs supported by the uniquely mapped reads from SAM files and obtained a polyadenylation tag (PAT) file using an in-house script. After that, we merged all the PAT files to determine the final PASs for all samples. PASs within 25 nucleotides of one another were grouped into one polyadenylation site cluster (PAC) using GetPolyaSiteCluster<sup>33</sup>. PACs with few reads were rejected according to different criteria depending on library size. For libraries that had less than 1.7M reads, clusters were retained only if a group of 5 biological replicates had at least 3 samples with  $\geq 3$  reads. For libraries with more than 1.7M reads, at least 3 samples with  $\geq 4$  reads were required.

**Gene annotation and usage of poly(A) sites.** We annotated all the final PACs for PAS\_ID, gene symbol, functional region, and other factors, as indicated, using Cuffcompare (v2.2.1)<sup>34</sup>, Perl scripts, and annotation file (GCF\_000001895.5\_Rnor\_6.0\_genomic.gtf; <https://ftp.ncbi.nlm.nih.gov/>). Clusters that mapped to mitochondrial genes were removed, then the number of PAS-covered reads was normalized<sup>35</sup> to the total number of covered reads within each library and rescaled by a factor of  $10^7$ .

**Circadian/ultradian PAS discovery.** Using unnormalized PAS read counts as input, rhythmic patterns were identified using the MetaCycle<sup>36</sup> R package meta2d, which synthesizes the results of three cycle analysis algorithms (ARSER, JTK\_Cycle, and Lomb-Scargle). The analysis was run 5 times with different replicates inserted into each of the appropriate ZT time slots, and the average  $p$ -value, FDR, phase, and other statistics were calculated. Only the highly corroborated PASs that were significant ( $p < 0.05$ ) in all 5 trials were used for all analyses. Plots of read counts use normalized reads per  $10^7$  and show the SEM of 5 biological replicates.

**Detailed mapping of APA sites.** The data supporting all figures depicting APA sites was from rat genome build BN7.2 and the UCSC (<http://genome.ucsc.edu>) and RDG (<https://rgd.mcw.edu/rgdweb/homepage/>) genome browsers<sup>37,38</sup>.)

**Gene ontology and pathway analysis.** Gene over-representation analysis was performed with the web-based tool WebGestalt<sup>39</sup>. Input gene symbol sets representing genes with cycling APA sites ( $p < 0.05$  in 5 of 5 trials and  $> 1$  PAS) or APA sites that were differentially expressed with sleep pressure ( $p < 0.01$ ,  $\log_2FC > 0.5$  and  $> 1$  PAS), were compared to relevantly annotated rat genes using an output threshold of  $FDR \leq 0.05$ . For phase-specific analysis, a sliding window of 5 h centered on each sample collection timepoint was used. For example, for phase ZT6, all PASs with average phase calculations that ranged from 3.5 to 8.5 were grouped.

**Differential expression analysis of sleep deprivation/recovery.** To evaluate the expression of PASs in sleep homeostasis experiments, PAS counts from rats recovering from 6 h SD were contrasted with time-matched controls (R0 vs ZT6, R2 vs ZT8, R4 vs ZT10, R8 vs ZT14). We removed high variation from the first principal component systematically, resulting in improved variance estimates for low read counts. Prcomp (in R) was used to perform principal component analysis (PCA) and to find eigenvectors by way of singular value decomposition. DESeq-2 with "Apeglm" Shrinkage<sup>40</sup> and the Wald Test were used to generate test statistics in R software. The FDRtool was used to determine the Local FDR.

## RESULTS

**Identification of PASs in the rat forebrain.** In order to identify changes in PAS usage, replicate circadian samples (central forebrains) were taken from five rats every four hours starting at two hours after lights on (i.e., ZT2, ZT6, ZT10, ZT14, ZT18 and ZT22) (Fig. 1a, b). RNA was purified from these samples and used to generate WTTs-seq cDNA libraries that were subsequently sequenced. Poly(A)-directed sequence reads were then mapped to the rat genome, giving rise to 31,796 PAS clusters (see Supplementary Table S1). All mitochondrial PASs were removed since some of them constituted a large fraction of the total reads. Among the 31,757 non-mitochondrial PAS clusters identified, a sizable portion mapped to unannotated or intergenic regions, leaving 26,635 PASs that mapped to named loci (i.e., genes). Many APAs occur at different points within the longest 3' UTR (Fig. 1c, sites 4 and 5). Some are distal to the longest documented 3' UTR (site 6), while some occur in internal exons (site 1) or introns (sites 2 and 3) (Fig. 1c). In our data set of all PASs that mapped to genes, 45% mapped to genes with  $\geq 2$  APA sites, and 19% mapped to genes with  $\geq 3$  APA sites (Fig. 1d). The average number of APA sites per gene was 1.9.

**Identification of PASs that exhibit a daily cycle.** Periodicity of PAS expression was assessed using meta2<sup>36</sup>. Circadian (24 h period) oscillations were demonstrated for 2,011 PASs. Among these, 1,173 were in genes with  $\geq 2$  total APA sites, including ones in known diurnal transcripts, such as *Dbp* (circadian in 2 of 2 APA sites recovered), *Nr1d2* (in 1 of 1), *Per2* (in 2 of 2), and *Ntrk2* (in 2 of 10)<sup>41</sup> (Table 1 and Supplementary Table S2).

To look for functions or cell components that are particularly affected by APA site usage in a time-of-day dependent manner, we performed pathway and gene ontology (GO) over-representation analyses using the online tool WebGestalt<sup>39</sup>. The set of 1,173 gene symbols corresponding to circadian PASs in genes

with  $\geq 2$  APAs were input (Table 2 and Supplementary Table S3). Glutamatergic Synapse, Membrane Trafficking and Circadian Entrainment are among the enriched terms.

We were interested whether circadian APAs might cluster predominantly into certain phases of peak expression, and whether APAs that share a common peak phase might also share some functional relationship. When circadian APAs from genes with  $\geq 2$  total APAs were grouped by phase, it was evident that some phases had very few APAs relative to other phases and the expression levels of many APAs peaked around ZT20 (Supplementary Fig. S1). GO and pathway analysis on each group and found that only phases 2, 10 and 18 had significantly over-represented terms. Phase 18 had the most, with the over-representation of multiple signaling pathways, including 'neuron to neuron synapse' and 'post-synaptic specialization' (Supplementary Table S4).

The realization that rhythms shorter than 24h are biologically important is growing<sup>42-46</sup>. Thus, we evaluated the PASs data for ultradian cycling using meta2d with the period set to 12 h. Overall, 1502 PASs that cycled with a 12 h period were identified (Supplementary Table S5). Of the 12 h cycling PASs, 1,198 were in genes, and after adjusting for genes with multiple 12h cycling APAs, there were 1,149 unique genes in the set. In total, 827 of the 12 h cycling APA sites were in genes that had  $\geq 2$  APAs, representing 778 unique genes. Pathway analysis on this set of 778 unique genes (Supplementary Table S6) showed that CREB phosphorylation and circadian entrainment were highly enriched, while GO analysis of this data set resulted in 16 GO terms related to the synapse.

**PASs are differentially expressed after sleep deprivation and during recovery sleep.** To investigate changes in APA site usage related to sleep pressure, rats were subjected to SD for 6 h from ZT0 to ZT6, and central forebrain tissue was collected immediately afterwards (R0). Additional animals were allowed to recover for 2, 4, or 8 h after SD (R2, R4 and R8) before tissue was collected. WTTS-seq data from these samples were compared to time-matched controls that were allowed to sleep undisturbed (ZT6, ZT8, ZT10 and ZT14). All groups consisted of 5 biological replicates. Our sequencing data showed that the most significant differences in expression were seen when we compared R0 with its control (ZT6) and R4 with its control (ZT10) (Supplementary Table S7 and Fig. 2). Interestingly, a *Homer1a* APA isoform is the most abundant at ZT6, ZT10 and R0, whereas a full-length isoform is dominant at ZT10 (Supplementary Fig. S2 a and b) Also, the expression of one APA isoform of *Prmt1*, was upregulated with high confidence in the ZT6 vs R0 (Fig. 2). PRMT1 protein regulates multiple stress response pathways<sup>47,48</sup>.

The gene names of differentially expressed APA sites from genes with  $\geq 2$  APAs were used for GO and pathway over-representation analysis (Table 3). ZT6 vs R0 only had significant results for GO while ZT10 vs R4 had significant GO and pathway results.

**Comparison of APA-linked brain disorder susceptibility genes with WTTS-seq identified circadian APAs and APAs differentially expressed with sleep pressure.** A recent survey by Cui et al.<sup>30</sup> using APA transcriptome-wide association studies (TWAS) highlighted the importance of APA site usage in brain disorders. To establish the extent to which genes with APA-linked neurological phenotypes had circadian

or sleep related changes in rats, our list of circadian genes with  $\geq 2$  APA sites was compared to those reported in Cui et al.<sup>30</sup>. There were 25 overlapping genes (representing 28 APAs in our data, since three genes had 2 circadian APA sites). Another 19 genes with WTTS-seq-identified APA sites that cycle on a 12 h period were identified in the TWAS data set, as were nine genes (11 APA sites) that were differentially expressed with sleep pressure. Altogether, 54 APAs representing 46 genes were observed in common with genes having disease-associated APAs (Table 4).

## Discussion

APA site usage is an understudied aspect of gene regulation. Although APA sequencing can reveal changes in overall gene expression, it's designed to focus on changes in APA usage and cannot reveal differences in splicing or transcription start sites (TSSs). On the other hand, bulk RNA-seq analysis often ignores APA, TSS and splice isoforms to simply assess reads per gene. Currently it would be very difficult to enumerate copies of all the mRNA isoforms for each gene. Yet appreciation is growing for the importance of APA sites in regulating mRNA stability<sup>16,49</sup>, mRNA/protein localization<sup>19,50,51</sup>, and human disease<sup>30,52</sup>.

Rhythmic APA site usage has been uncovered in the mouse liver<sup>21,22,53</sup>, and in temperature-entrained cultured cells, circadian APA usage occurs in many genes and can regulate expression of specific central clock genes<sup>23</sup>. Still, alternative poly(A) site usage hasn't been given enough attention. We therefore initiated this investigation into the conjunction of APA with sleep and circadian expression. As far as we are aware, the current study is the first to examine APA sites related to circadian rhythms and sleep pressure in any mammalian brain. In our analysis, we found 5,122 PASs and 318 circadian PASs that mapped outside of known genes, and many APAs within genes mapped to regions in which 3' ends have yet to be annotated. Based on prior WTTS-seq data sets and other PAS mapping approaches, we expect that some portion of our PASs will be method-based artifacts<sup>26,54</sup>, but, overall, the newly discovered PASs should add valuable insights into regulation of the rat transcriptome and for characterizing PAS usage in the mammalian brain. There are several, diverse ways in which data from this study can translate into biological relevance as described in the examples below.

Here, we observed that 6% of all PASs cycled with a 24 h period. One of the top pathways identified for the circadian APA gene set was 'circadian entrainment' (Table 2). Since transcription-translation feedback loops are central to circadian regulation, this may not be surprising, but APA site usage may well have a role<sup>23,53</sup>. For example, we find that one *Sin3b* APA is circadian (Fig 3a, b). *Sin3b* encodes short and long variants conserved in mammals. The short variant binds to CRY1 but cannot bind HDAC1<sup>55</sup>. The long isoform is implicated in regulation of *Per1/Per2* transcription<sup>56</sup>, along with many other genes<sup>57</sup>. In our data, long *Sin3b* APA reads constitute the predominant isoform at ZT6 and ZT22, while the short, circadian isoform is the most abundant one at ZT10, ZT14 and perhaps ZT2 (Fig 3b). *Sin3b* transcript levels in mouse hippocampus have previously been reported to be affected by sleep deprivation<sup>58</sup>, although this effect was not observed using TRAP-seq<sup>59</sup>, suggesting post-transcriptional processing can



lead to changes in sleep-dependent differential expression. Together with our work, this example highlights the importance of utilizing various -omic approaches to properly decipher the complexity of molecular processing tied to changes in behavioral state in the brain.

Additional significant pathways emerged from the circadian APAs, such as Oxytocin, Ephrin, and MAPK signaling that have demonstrated links to the circadian clock<sup>60-62</sup>. In the GO analysis of the circadian genes with multiple PASs, we discovered that terms related to the synapse (12), protein localization (6), and vesicles (7) (Table 2 and Supplementary Table S3) were enriched suggesting APAs are poised to affect neural communication.

A large proportion of circadian APAs had expression peaks around ZT20 (Supplementary Fig. S1). Considering that rats are nocturnal, this is similar to what has been seen for bulk transcripts in several human tissues, including brain<sup>63</sup>. Interestingly, among the identified circadian APA sites, 3 were in genes for RNA-binding proteins (*Celf2*, *Elavl3*, and *Rbfox1*) whose expressions correlate with more distal APA usage<sup>47</sup>. Peak expression of these three genes is from ZT21 to ZT1, so it would be interesting to see if transcripts of predicted targets tend to be longer at these times.

In addition to the 24 h circadian rhythm, recent studies have also demonstrated the existence of cell-autonomous ultradian clocks that run independently of the circadian clock to regulate 12 h oscillations in gene expression and metabolism<sup>42-46</sup>. Here we found that 5% of all PASs cycle with a 12 h period. Further analysis of these genes showed enrichment of gene ontology terms and pathways such as "regulation of trans-synaptic signaling" and "protein-protein interactions at synapses" (Supplementary Table S6), indicating that APAs could function to regulate cyclic actions of cell signaling and communication.

Gene expression studies following changes in sleep homeostasis have largely ignored alternative polyadenylation. Of the 31,795 total PASs characterized in rat forebrain in our study, we determined that 2.5% were differentially expressed with sleep deprivation and recovery sleep. We also observed 6 GO terms significantly enriched following 6 hours of sleep loss and 26 following 4 hours of recovery sleep (Table 3).

Human APA isoforms have been linked to many neurological disorders<sup>30</sup>. Among the genes that we identified to have rhythmic expression of APA sites or had APA sites that were affected by sleep pressure, we found that 46 have also been correlated with brain disorder susceptibility (Table 4). For example, the human *MAPT/TAU* gene produces transcripts containing short or long 3' UTRs, and a 3' SNP is associated with both 3' UTR length and risks for 8 neurological disorders, including Alzheimer's and Parkinson's diseases<sup>30</sup>. Homozygosity of the more common SNP variant is associated with short *MAPT* 3' UTRs, homozygosity of the less common SNP variant is associated with long 3' UTRs, and heterozygosity is associated with 3' UTRs of intermediate lengths. In our rat APA data, there were both short and long 3' UTR forms (5 in total) of the *Mapt* gene that were identified (Fig. 3c, d). Only two are currently annotated in the rat genome and one of the newly discovered APAs was observed to cycle with time-of-day. In mouse, binding of the ALS-associated protein TDP-43 to two sites in the 3' UTR of *Mapt*

has been shown to destabilize the mRNA<sup>64</sup>. In Alzheimer's disease, the expression level of TDP-43 protein is often low, and TAU is overexpressed and eventually forms neurofibrillary tangles. The two TDP-43 binding sites that were experimentally determined in mouse are conserved in sequence and position in the rat gene, implying that transcripts with shorter 3' UTRs would not be affected by TDP-43, while longer ones could be destabilized<sup>64,65</sup>. The presence of at least one putative TDP-43 binding site in the human MAPT 3'UTR suggests that this may be contributing to the neurological disorder risk.

*Ntrk2* is among the APA TWAS genes linked to anxiety<sup>30</sup> and has been associated with autism in other studies<sup>66</sup>. We found strong circadian oscillations of the 2 most abundant APA sites of the short, tyrosine kinase deficient (TK-) *Ntrk2* isoform. The TK- isoform of *Ntrk2* has several known functions, including a dominant negative effect on the full-length TK+ isoform during neuronal proliferation, differentiation, and survival. In addition, the TK- version promotes filopodia and neurite outgrowth; sequesters, translocates, and presents BDNF; and affects calcium signaling and cytoskeletal modifications in glia<sup>67</sup>. Our WTTS-seq data revealed short, medium, and long 3' UTRs in the rat *Ntrk2* TK- isoform (Fig. 3e). In mice, the longer *Ntrk2* TK- transcripts are preferentially targeted to apical dendrites<sup>68</sup>. Since the sequence of the rat 3' UTR is highly conserved with the mouse sequence, it is plausible that an analogous dendritic localization mechanism is also in use in the rat (Fig. 2c). Interestingly, 'Ntrk signaling' was one of the pathways over-represented in the circadian APA genes (Supplementary Table S3). APA sites in *Src*, *Frs2*, *Atf1*, *Nras*, *Sh3gl2*, *Ntrk3*, *Mapk1*, *Grb2*, *Pik3r1*, and *Mapk14* contributed to this enrichment.

Four different APAs from the *Sorl1* gene exhibited significant changes in our analyses; two circadian, one cycled with a 12 h period, and one was reduced during recovery from sleep deprivation (Fig. 4). In total, there were seven APAs in the *Sorl1* 3'UTR, three short, one medium and two long. The longest and most abundant isoform cycles per 12 h, the second longest and medium ones are circadian and the shortest isoform is differentially expressed after SD (Fig. 4). The mouse and human 3' UTRs share extensive similarities including 5 APAs in mouse and 3 in human based on the PolyA\_DB v3 ([https://exon.apps.wistar.org/polya\\_db/v2/](https://exon.apps.wistar.org/polya_db/v2/)) and UCSC database<sup>37</sup>. Four microRNA binding sites with high probability of preferential conservation are in good alignment (TargetScanHuman v8.0)<sup>69</sup>. The first motif can be bound by five miRNAs (miR-25-3p, miR-32-5p, miR-92-3p, miR-363-3p, and miR-367-3p), while the second contains overlapping 7mer and 8mer motifs bound by miR-128-3p and miR-27-3p, respectively. The final two more distal sites are recognized by miR-153-3p and mir-137 (Fig. 4a). Sequences matching the consensus binding site for CPEB are present in the 3' UTRs of all three species, with 2 in very good alignment. Cytoplasmic polyadenylation element binding protein (CPEB) facilitates mRNA trafficking to synapses and local translation<sup>70,71</sup>, and we have previously shown that the core clock-controlled *Fabp7* mRNA<sup>72,73</sup> contains functional CPE sites in its 3'UTR to regulate translation<sup>74</sup>. Since APOE4, an apolipoprotein E variant with increased risk of AD<sup>75</sup>, disrupts FABP7 interaction with sortilin, (an APOE receptor similar to *Sorl1*), to interfere with neuroprotective lipid signaling<sup>76</sup>, this suggests circadian variation in local translation of CPEB-mediated polyadenylation of target mRNAs may be a generalizable mechanism that modulates AD susceptibility through downstream lipid pathways. Any

one or more of these conserved features could lead to conserved functional consequences dependent on APA choice. SORL1 encodes an endosomal recycling receptor<sup>77</sup>. Many polymorphisms or a deficiency of the gene are strong risk factors for AD<sup>78,79</sup>.

Although the current data are correlational in nature, they leverage a call to action for additional work to elucidate the core mechanisms of PAS usage in the brain and to examine the capacity of APA to affect the transcriptomes and proteomes that regulate central brain processes known to be altered by time-of-day and sleep/wake homeostasis. Moreover, it is known that PAS usage varies across brain region and cell type<sup>20</sup> (i.e., substructure-, circuit-, laminar- or nucleus-specific)<sup>80</sup>. These hypothesis-generating data provide an impetus for continued research aimed at delineating how sleep and circadian rhythms impact mental health and neurodegenerative disease.

## Declarations

### Data Availability

The PAS sequence data discussed here have been deposited in NCBI's Gene Expression Omnibus<sup>81</sup> and are accessible through GEO Series accession number GSE250324 (<https://www.ncbi.nlm.nih.gov/geo/query/acc.cgi?acc=GSE250324>).

### Acknowledgements

The authors would also like to thank Michelle Schmidt, Jennifer J. Michal, Kyle C. Schuppe, Vivian Wei, and Brooke Rogers for technical assistance, and Amy Sullivan for an expert and detailed critique of the manuscript.

### Author Contribution

C.D. and J.G. conceived of and designed the experiments. C.D. collected the samples.

C.F. wrote the main manuscript text and prepared figures and tables. H.W. processed the sequence data, (mapping, clustering and APA annotation). N.P and A.D. carried out differential expression analyses. J.G., C.D., C.F., Z.J. and J.D. revised the manuscript. C.D. and J.G. funded the study. All authors reviewed and approved the final version of the manuscript.

### Funding

This work was supported by NIH grant R35GM133440 "Characterizing evolutionarily conserved mechanisms underlying sleep, clocks, and memory", and initial seed funds provided by the Department of Translational Medicine and Physiology, WSU.

### Competing interests

J.G. is the founder of Blood Brain Biotechnology, LLC. All other authors declare no competing interests.

# References

1. Abbott, S. M., Malkani, R. G. & Zee, P. C. Circadian disruption and human health: A bidirectional relationship. *Eur J Neurosci* **51**, 567-583, doi:10.1111/ejn.14298 (2020).
2. Grandner, M. A. & Fernandez, F. X. The translational neuroscience of sleep: A contextual framework. *Science* **374**, 568-573, doi:10.1126/science.abj8188 (2021).
3. Medic, G., Wille, M. & Hemels, M. E. Short- and long-term health consequences of sleep disruption. *Nat Sci Sleep* **9**, 151-161, doi:10.2147/NSS.S134864 (2017).
4. Baglioni, C. *et al.* Sleep and mental disorders: A meta-analysis of polysomnographic research. *Psychol Bull* **142**, 969-990, doi:10.1037/bul0000053 (2016).
5. Alachkar, A. *et al.* The hidden link between circadian entropy and mental health disorders. *Transl Psychiatry* **12**, 281, doi:10.1038/s41398-022-02028-3 (2022).
6. Logan, R. W. & McClung, C. A. Rhythms of life: circadian disruption and brain disorders across the lifespan. *Nat Rev Neurosci* **20**, 49-65, doi:10.1038/s41583-018-0088-y (2019).
7. Musiek, E. S. & Holtzman, D. M. Mechanisms linking circadian clocks, sleep, and neurodegeneration. *Science* **354**, 1004-1008, doi:10.1126/science.aah4968 (2016).
8. Krueger, J. M., Frank, M. G., Wisor, J. P. & Roy, S. Sleep function: Toward elucidating an enigma. *Sleep Med Rev* **28**, 46-54, doi:10.1016/j.smrv.2015.08.005 (2016).
9. Krueger, J. M. & Tononi, G. Local use-dependent sleep; synthesis of the new paradigm. *Curr Top Med Chem* **11**, 2490-2492, doi:10.2174/156802611797470330 (2011).
10. Anafi, R. C., Kayser, M. S. & Raizen, D. M. Exploring phylogeny to find the function of sleep. *Nat Rev Neurosci* **20**, 109-116, doi:10.1038/s41583-018-0098-9 (2019).
11. Siegel, J. M. Sleep function: an evolutionary perspective. *Lancet Neurol* **21**, 937-946, doi:10.1016/S1474-4422(22)00210-1 (2022).
12. Panda, S., Hogenesch, J. B. & Kay, S. A. Circadian rhythms from flies to human. *Nature* **417**, 329-335, doi:10.1038/417329a (2002).
13. Cirelli, C. The genetic and molecular regulation of sleep: from fruit flies to humans. *Nat Rev Neurosci* **10**, 549-560, doi:10.1038/nrn2683 (2009).
14. Lane, J. M. *et al.* Genetics of circadian rhythms and sleep in human health and disease. *Nat Rev Genet* **24**, 4-20, doi:10.1038/s41576-022-00519-z (2023).
15. Jagannath, A., Taylor, L., Wakaf, Z., Vasudevan, S. R. & Foster, R. G. The genetics of circadian rhythms, sleep and health. *Hum Mol Genet* **26**, R128-R138, doi:10.1093/hmg/ddx240 (2017).
16. Mitschka, S. & Mayr, C. Context-specific regulation and function of mRNA alternative polyadenylation. *Nat Rev Mol Cell Biol* **23**, 779-796, doi:10.1038/s41580-022-00507-5 (2022).
17. Tian, B. & Manley, J. L. Alternative polyadenylation of mRNA precursors. *Nat Rev Mol Cell Biol* **18**, 18-30, doi:10.1038/nrm.2016.116 (2017).

18. Mayr, C. Evolution and Biological Roles of Alternative 3'UTRs. *Trends Cell Biol* **26**, 227-237, doi:10.1016/j.tcb.2015.10.012 (2016).
19. Arora, A. *et al.* The Role of Alternative Polyadenylation in the Regulation of Subcellular RNA Localization. *Front Genet* **12**, 818668, doi:10.3389/fgene.2021.818668 (2021).
20. Kang, B. *et al.* Infernape uncovers cell type-specific and spatially resolved alternative polyadenylation in the brain. *Genome Res*, doi:10.1101/gr.277864.123 (2023).
21. Greenwell, B. J. *et al.* Isoform-specific regulation of rhythmic gene expression by alternative polyadenylation. *bioRxiv*, doi:10.1101/2020.12.12.422514 (2020).
22. Gendreau, K. L., Unruh, B. A., Zhou, C. & Kojima, S. Identification and Characterization of Transcripts Regulated by Circadian Alternative Polyadenylation in Mouse Liver. *G3 (Bethesda)* **8**, 3539-3548, doi:10.1534/g3.118.200559 (2018).
23. Liu, Y. *et al.* Cold-induced RNA-binding proteins regulate circadian gene expression by controlling alternative polyadenylation. *Sci Rep* **3**, 2054, doi:10.1038/srep02054 (2013).
24. Gruber, A. J. & Zavolan, M. Alternative cleavage and polyadenylation in health and disease. *Nat Rev Genet* **20**, 599-614, doi:10.1038/s41576-019-0145-z (2019).
25. Chen, W. *et al.* Alternative Polyadenylation: Methods, Findings, and Impacts. *Genomics Proteomics Bioinformatics* **15**, 287-300, doi:10.1016/j.gpb.2017.06.001 (2017).
26. Zhou, X. *et al.* Accurate Profiling of Gene Expression and Alternative Polyadenylation with Whole Transcriptome Termini Site Sequencing (WTTS-Seq). *Genetics* **203**, 683-697, doi:10.1534/genetics.116.188508 (2016).
27. Brutman, J. N. *et al.* Vapor Cannabis Exposure Promotes Genetic Plasticity in the Rat Hypothalamus. *Sci Rep* **9**, 16866, doi:10.1038/s41598-019-53516-4 (2019).
28. Mohanan, N. K., Shaji, F., Koshre, G. R. & Laishram, R. S. Alternative polyadenylation: An enigma of transcript length variation in health and disease. *Wiley Interdiscip Rev RNA* **13**, e1692, doi:10.1002/wrna.1692 (2022).
29. Mittleman, B. E. *et al.* Alternative polyadenylation mediates genetic regulation of gene expression. *Elife* **9**, doi:10.7554/eLife.57492 (2020).
30. Cui, Y. *et al.* Alternative polyadenylation transcriptome-wide association study identifies APA-linked susceptibility genes in brain disorders. *Nat Commun* **14**, 583, doi:10.1038/s41467-023-36311-8 (2023).
31. Strobel, B. K., Schmidt, M. A., Harvey, D. O. & Davis, C. J. Image discrimination reversal learning is impaired by sleep deprivation in rats: Cognitive rigidity or fatigue? *Front Syst Neurosci* **16**, 1052441, doi:10.3389/fnsys.2022.1052441 (2022).
32. Ward, C. P., Wooden, J. I. & Kieltyka, R. Effects of Sleep Deprivation on Spatial Learning and Memory in Juvenile and Young Adult Rats. *Psychol Neurosci* **10**, 109-116, doi:10.1037/pne0000075 (2017).
33. Dong, M., Ji, G., Li, Q. Q. & Liang, C. Extraction of poly(A) sites from large-scale RNA-Seq data. *Methods Mol Biol* **1255**, 25-37, doi:10.1007/978-1-4939-2175-1\_3 (2015).

34. Trapnell, C. *et al.* Differential gene and transcript expression analysis of RNA-seq experiments with TopHat and Cufflinks. *Nat Protoc* **7**, 562-578, doi:10.1038/nprot.2012.016 (2012).
35. Wang, H. *et al.* Genome-Wide Analysis and Functional Characterization of the Polyadenylation Site in Pigs Using RNAseq Data. *Sci Rep* **6**, 36388, doi:10.1038/srep36388 (2016).
36. Wu, G., Anafi, R. C., Hughes, M. E., Kornacker, K. & Hogenesch, J. B. MetaCycle: an integrated R package to evaluate periodicity in large scale data. *Bioinformatics* **32**, 3351-3353, doi:10.1093/bioinformatics/btw405 (2016).
37. Nassar, L. R. *et al.* The UCSC Genome Browser database: 2023 update. *Nucleic Acids Res* **51**, D1188-D1195, doi:10.1093/nar/gkac1072 (2023).
38. Vedi, M. *et al.* 2022 updates to the Rat Genome Database: a Findable, Accessible, Interoperable, and Reusable (FAIR) resource. *Genetics* **224**, doi:10.1093/genetics/iyad042 (2023).
39. Liao, Y., Wang, J., Jaehnig, E. J., Shi, Z. & Zhang, B. WebGestalt 2019: gene set analysis toolkit with revamped UIs and APIs. *Nucleic Acids Res* **47**, W199-W205, doi:10.1093/nar/gkz401 (2019).
40. Zhu, A., Ibrahim, J. G. & Love, M. I. Heavy-tailed prior distributions for sequence count data: removing the noise and preserving large differences. *Bioinformatics* **35**, 2084-2092, doi:10.1093/bioinformatics/bty895 (2019).
41. Bova, R., Micheli, M. R., Qualadrucci, P. & Zucconi, G. G. BDNF and trkB mRNAs oscillate in rat brain during the light-dark cycle. *Brain Res Mol Brain Res* **57**, 321-324, doi:10.1016/s0169-328x(98)00092-8 (1998).
42. Zhu, B. *et al.* A Cell-Autonomous Mammalian 12 hr Clock Coordinates Metabolic and Stress Rhythms. *Cell Metab* **25**, 1305-1319.e1309, doi:10.1016/j.cmet.2017.05.004 (2017).
43. Pan, Y. *et al.* 12-h clock regulation of genetic information flow by XBP1s. *PLoS Biol* **18**, e3000580, doi:10.1371/journal.pbio.3000580 (2020).
44. Meng, H. *et al.* XBP1 links the 12-hour clock to NAFLD and regulation of membrane fluidity and lipid homeostasis. *Nat Commun* **11**, 6215, doi:10.1038/s41467-020-20028-z (2020).
45. Tang, M. *et al.* An extra-clock ultradian brain oscillator sustains circadian timekeeping. *Sci Adv* **8**, eabo5506, doi:10.1126/sciadv.abo5506 (2022).
46. Asher, G. & Zhu, B. Beyond circadian rhythms: emerging roles of ultradian rhythms in control of liver functions. *Hepatology* **77**, 1022-1035, doi:10.1002/hep.32580 (2023).
47. Yuniati, L. *et al.* Tumor suppressor BTG1 promotes PRMT1-mediated ATF4 function in response to cellular stress. *Oncotarget* **7**, 3128-3143, doi:10.18632/oncotarget.6519 (2016).
48. Giambruno, R. & Bonaldi, T. Dual role of PRMT1-dependent arginine methylation in cellular responses to genotoxic stress. *Mol Cell Oncol* **7**, 1743808, doi:10.1080/23723556.2020.1743808 (2020).
49. Stacey, S. N. *et al.* A germline variant in the TP53 polyadenylation signal confers cancer susceptibility. *Nat Genet* **43**, 1098-1103, doi:10.1038/ng.926 (2011).
50. Cheng, L. C. *et al.* Alternative 3' UTRs play a widespread role in translation-independent mRNA association with the endoplasmic reticulum. *Cell Rep* **36**, 109407, doi:10.1016/j.celrep.2021.109407

(2021).

51. Farberov, L. *et al.* Multiple Copies of microRNA Binding Sites in Long 3'UTR Variants Regulate Axonal Translation. *Cells* **12**, doi:10.3390/cells12020233 (2023).
52. Griesemer, D. *et al.* Genome-wide functional screen of 3'UTR variants uncovers causal variants for human disease and evolution. *Cell* **184**, 5247-5260.e5219, doi:10.1016/j.cell.2021.08.025 (2021).
53. Ptitsyna, N., Boughorbel, S., El Anbari, M. & Ptitsyn, A. The role of alternative Polyadenylation in regulation of rhythmic gene expression. *BMC Genomics* **18**, 576, doi:10.1186/s12864-017-3958-1 (2017).
54. Balázs, Z. *et al.* Template-switching artifacts resemble alternative polyadenylation. *BMC Genomics* **20**, 824, doi:10.1186/s12864-019-6199-7 (2019).
55. Latypova, X. *et al.* Haploinsufficiency of the Sin3/HDAC corepressor complex member SIN3B causes a syndromic intellectual disability/autism spectrum disorder. *Am J Hum Genet* **108**, 929-941, doi:10.1016/j.ajhg.2021.03.017 (2021).
56. Naruse, Y. *et al.* Circadian and light-induced transcription of clock gene Per1 depends on histone acetylation and deacetylation. *Mol Cell Biol* **24**, 6278-6287, doi:10.1128/MCB.24.14.6278-6287.2004 (2004).
57. Naruse, Y., Aoki, T., Kojima, T. & Mori, N. Neural restrictive silencer factor recruits mSin3 and histone deacetylase complex to repress neuron-specific target genes. *Proc Natl Acad Sci U S A* **96**, 13691-13696, doi:10.1073/pnas.96.24.13691 (1999).
58. Vecsey, C. G. *et al.* Genomic analysis of sleep deprivation reveals translational regulation in the hippocampus. *Physiol Genomics* **44**, 981-991, doi:10.1152/physiolgenomics.00084.2012 (2012).
59. Lyons, L. C., Chatterjee, S., Vanrobaeys, Y., Gaine, M. E. & Abel, T. Translational changes induced by acute sleep deprivation uncovered by TRAP-Seq. *Mol Brain* **13**, 165, doi:10.1186/s13041-020-00702-5 (2020).
60. Caba, M. *et al.* Oxytocinergic cells of the posterior hypothalamic paraventricular nucleus participate in the food entrained clock. *Sci Rep* **11**, 19957, doi:10.1038/s41598-021-99266-0 (2021).
61. Kumar, J. R. *et al.* Relaxin' the brain: a case for targeting the nucleus incertus network and relaxin-3/RXFP3 system in neuropsychiatric disorders. *Br J Pharmacol* **174**, 1061-1076, doi:10.1111/bph.13564 (2017).
62. Goldsmith, C. S. & Bell-Pedersen, D. Diverse roles for MAPK signaling in circadian clocks. *Adv Genet* **84**, 1-39, doi:10.1016/B978-0-12-407703-4.00001-3 (2013).
63. Talamanca, L., Gobet, C. & Naef, F. Sex-dimorphic and age-dependent organization of 24-hour gene expression rhythms in humans. *Science* **379**, 478-483, doi:10.1126/science.add0846 (2023).
64. Gu, J. *et al.* TDP-43 suppresses tau expression via promoting its mRNA instability. *Nucleic Acids Res* **45**, 6177-6193, doi:10.1093/nar/gkx175 (2017).
65. Gu, J., Chu, D., Jin, N., Chen, F. & Liu, F. Cyclic AMP-Dependent Protein Kinase Phosphorylates TDP-43 and Modulates Its Function in Tau mRNA Processing. *J Alzheimers Dis* **70**, 1093-1102,

- doi:10.3233/JAD-190368 (2019).
66. Abdolmaleky, H. M., Martin, M., Zhou, J. R. & Thiagalingam, S. Epigenetic Alterations of Brain Non-Neuronal Cells in Major Mental Diseases. *Genes (Basel)* **14**, doi:10.3390/genes14040896 (2023).
  67. Fenner, B. M. Truncated TrkB: beyond a dominant negative receptor. *Cytokine Growth Factor Rev* **23**, 15-24, doi:10.1016/j.cytogfr.2012.01.002 (2012).
  68. Chen, S. *et al.* 3'UTRs Regulate Mouse Ntrk2 mRNA Distribution in Cortical Neurons. *J Mol Neurosci* **70**, 1858-1870, doi:10.1007/s12031-020-01579-8 (2020).
  69. McGear, S. E. *et al.* The biochemical basis of microRNA targeting efficacy. *Science* **366**, doi:10.1126/science.aav1741 (2019).
  70. Huang, Y. S., Carson, J. H., Barbarese, E. & Richter, J. D. Facilitation of dendritic mRNA transport by CPEB. *Genes Dev* **17**, 638-653, doi:10.1101/gad.1053003 (2003).
  71. Martin, K. C. & Zukin, R. S. RNA trafficking and local protein synthesis in dendrites: an overview. *J Neurosci* **26**, 7131-7134, doi:10.1523/JNEUROSCI.1801-06.2006 (2006).
  72. Gerstner, J. R. & Paschos, G. K. Circadian expression of Fabp7 mRNA is disrupted in Bmal1 KO mice. *Mol Brain* **13**, 26, doi:10.1186/s13041-020-00568-7 (2020).
  73. Vanderheyden, W. M., Fang, B., Flores, C. C., Jager, J. & Gerstner, J. R. The transcriptional repressor Rev-erba regulates circadian expression of the astrocyte Fabp7 mRNA. *Curr Res Neurobiol* **2**, doi:10.1016/j.crneur.2021.100009 (2021).
  74. Gerstner, J. R. *et al.* Time of day regulates subcellular trafficking, tripartite synaptic localization, and polyadenylation of the astrocytic Fabp7 mRNA. *J Neurosci* **32**, 1383-1394, doi:10.1523/JNEUROSCI.3228-11.2012 (2012).
  75. Kim, J., Basak, J. M. & Holtzman, D. M. The role of apolipoprotein E in Alzheimer's disease. *Neuron* **63**, 287-303, doi:10.1016/j.neuron.2009.06.026 (2009).
  76. Asaro, A. *et al.* ApoE4 disrupts interaction of sortilin with fatty acid-binding protein 7 essential to promote lipid signaling. *J Cell Sci* **134**, doi:10.1242/jcs.258894 (2021).
  77. Mishra, S. *et al.* The Alzheimer's gene SORL1 is a regulator of endosomal traffic and recycling in human neurons. *Cell Mol Life Sci* **79**, 162, doi:10.1007/s00018-022-04182-9 (2022).
  78. Andersen, O. M. *et al.* A genetically modified minipig model for Alzheimer's disease with SORL1 haploinsufficiency. *Cell Rep Med* **3**, 100740, doi:10.1016/j.xcrm.2022.100740 (2022).
  79. Lee, H. *et al.* Cell-type-specific regulation of APOE and CLU levels in human neurons by the Alzheimer's disease risk gene SORL1. *Cell Rep* **42**, 112994, doi:10.1016/j.celrep.2023.112994 (2023).
  80. Vanrobaeys, Y. *et al.* Spatial transcriptomics reveals unique gene expression changes in different brain regions after sleep deprivation. *Nat Commun* **14**, 7095, doi:10.1038/s41467-023-42751-z (2023).
  81. Edgar, R., Domrachev, M. & Lash, A. E. Gene Expression Omnibus: NCBI gene expression and hybridization array data repository. *Nucleic Acids Res* **30**, 207-210, doi:10.1093/nar/30.1.207 (2002).



# Tables

Tables 1 to 4 are available in the Supplementary Files section

# Figures

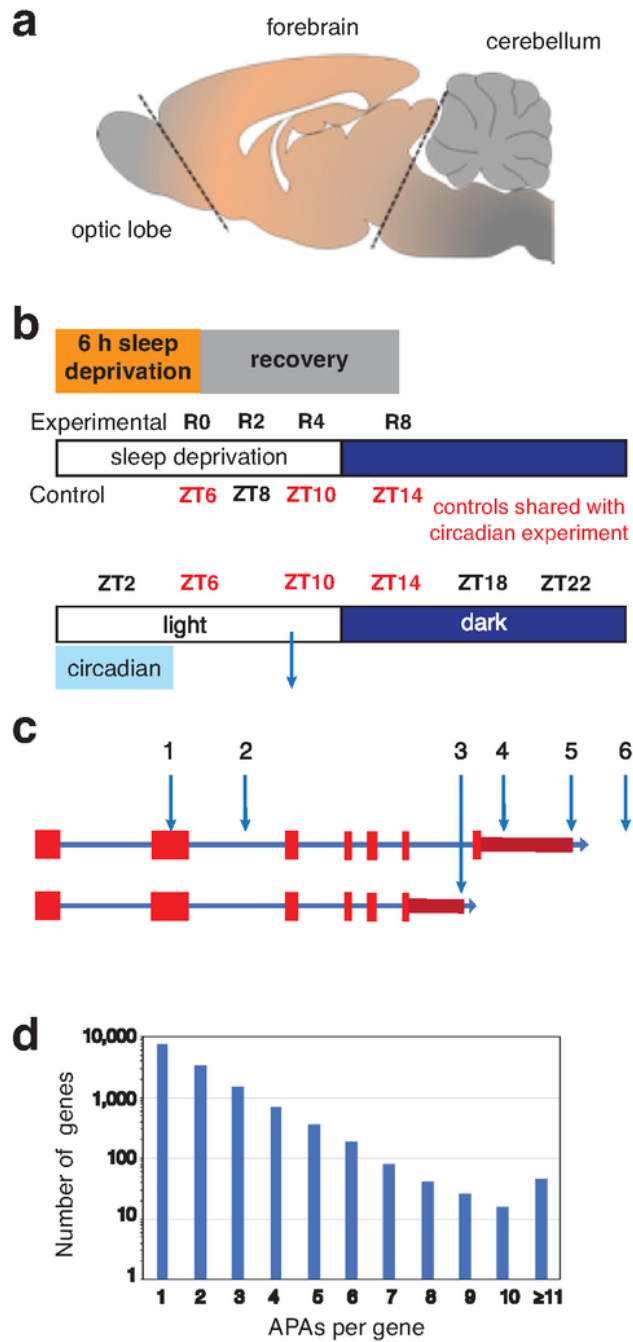
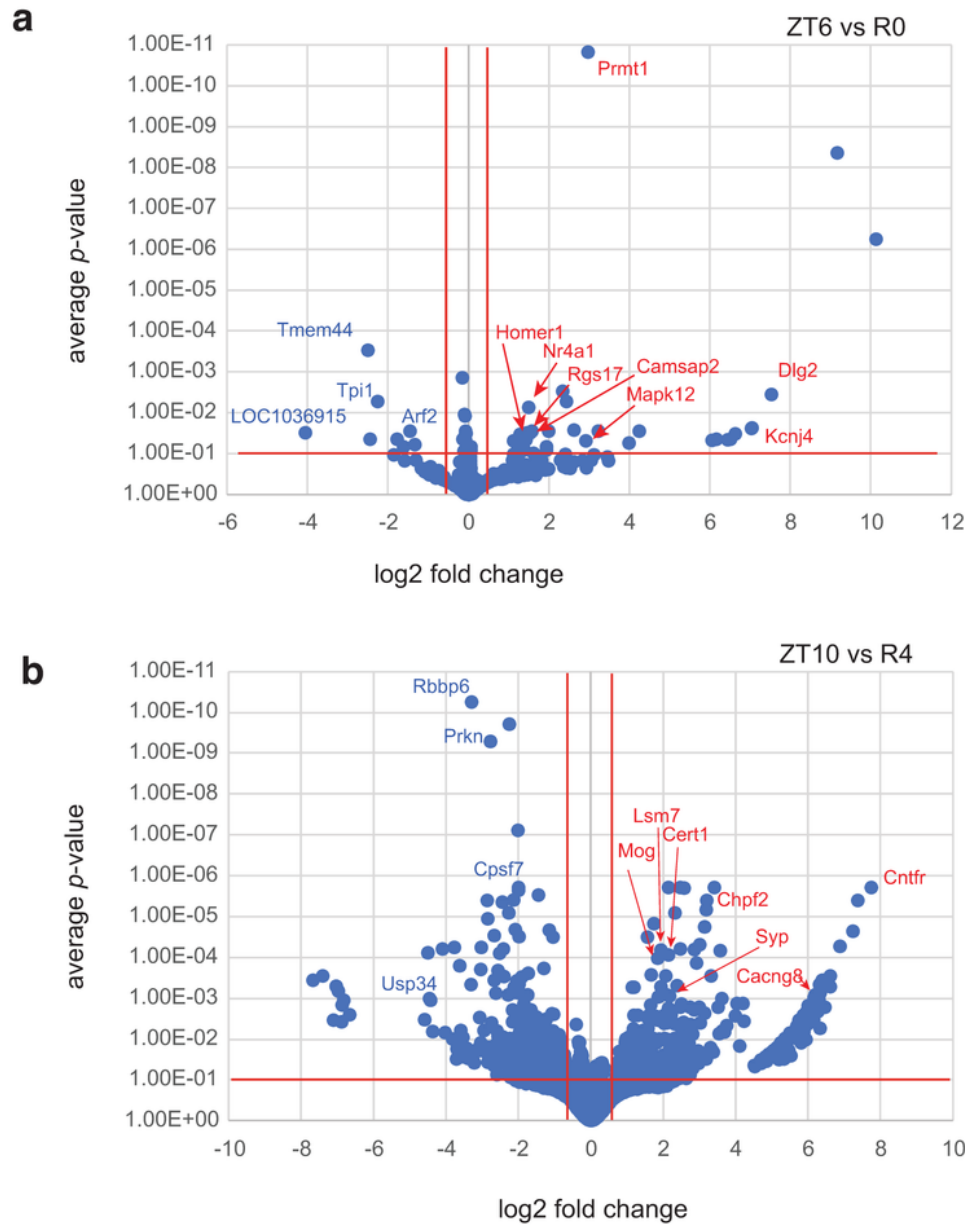


Figure 1

Schema of the brain region sampled, the collection time/condition, and a plot of the number of APA sites per gene. **(a)** The region of the central rat forebrain that was collected and used for RNA extraction is labeled 'forebrain'. **(b)** For sleep homeostasis experiments, rats were sleep-deprived for 6 h and allowed to recover for 0 to 8 h before tissue extraction. Three of the time-matched controls (no SD) were shared with the circadian experiment and one additional time point (no SD at ZT8), was not in common. For the circadian analysis, samples were taken at 4 h intervals from ZT2 until ZT22. Five biological replicates were used for all data points. **(c)** A diagram of a generic gene shows different types of APAs: within an internal exon (1); within an early intron (2); following an internal exon (3); within the longest documented 3' UTR (4); at the terminus of the longest documented 3' UTR (5); and distal to longest documented 3' UTR. **(d)** WTTS-seq PAS results; the number of genes on the x-axis (log<sub>10</sub> scale) are plotted against the number of APA sites per gene.



**Figure 2**

Differential expression of PASs by DESeq-2 with Apeglm Shrinkage. Log of adjusted  $p$ -values are plotted against log<sub>2</sub> fold changes from **(a)** ZT6 vs R0 and **(b)** ZT10 vs R4.

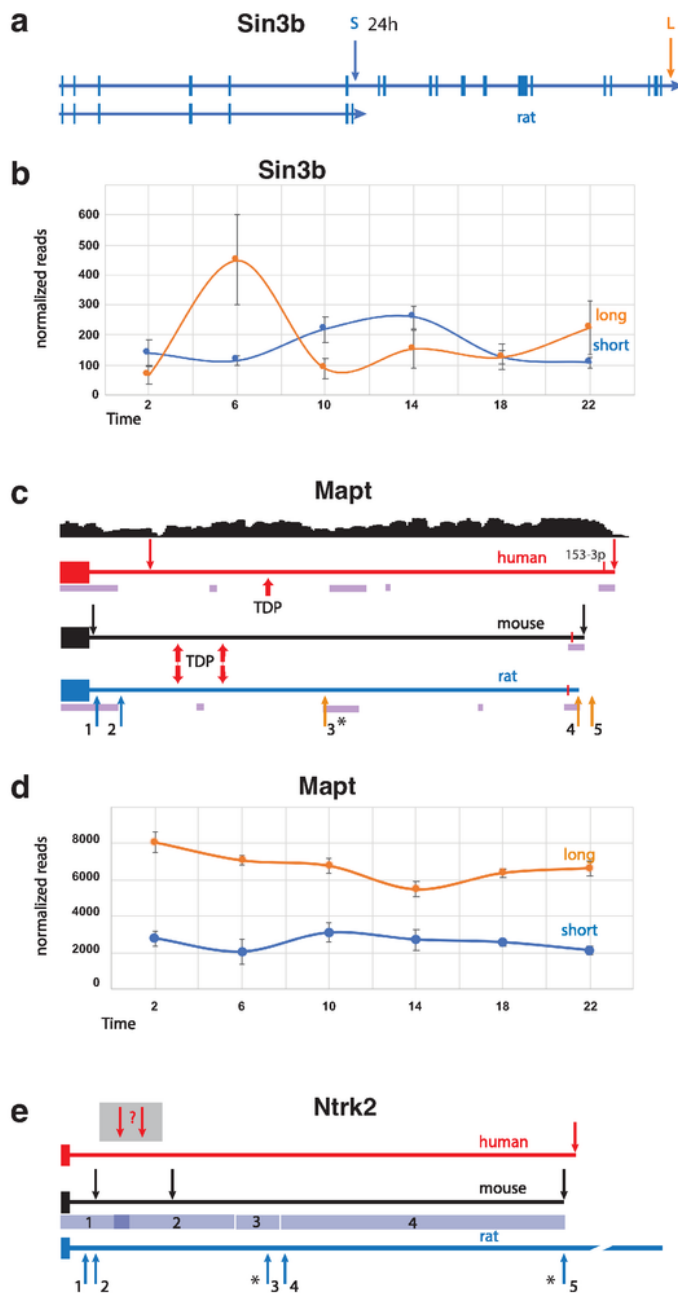


**Figure 3**

The *Sin3b* gene and 3' UTR regions of the *Mapt* and *Ntrk2* genes. **(a)** A map of the entire rat *Sin3b* gene depicts exons, introns and short and long APA sites. The corresponding genes in mouse and human are extremely similar. **(b)** The average normalized read counts  $\pm$ SE (y-axis) of the short (circadian) and long *Sin3b* APAs are plotted against time-of-day (x-axis). **(c)** Maps of the 3' UTR regions of the human, mouse, and rat *Mapt* genes are shown. Dark blue arrows indicate the positions of APA sites. In human *MAPT*,

APA usage correlates with several brain disorders. RNA-seq coverage from individuals homozygous for the less common SNP allele that is associated with longer transcripts (adapted from Cui. et al.<sup>27</sup>) is shown above the human *MAPT* 3' UTR map. Binding sites for TDP-43 (indicated by red arrows) that were experimentally determined in mouse align with putative sites in the rat gene, and one possible TDP-43 binding site is indicated in the human 3'UTR. The significantly circadian APA is marked with an asterisk. Blocks of homologous sequence between the rat and human genes that were found by BLAST search are indicated by purple bars. The 3' UTR lengths are 4,380, 4,119 and 3,946 n.t. for human, mouse, and rat, respectively. **(d)** The average normalized read counts  $\pm$ SE (y-axis) of the short *Mapt* isoforms lacking TDP binding sites (1+2) and the sum of the three longer isoforms (3+4+5) plotted against time-of-day (x-axis) are shown. **(e)** The 3' UTR of tyrosine kinase-deficient (TK-) isoforms of the human, mouse, and rat *Ntrk2* TK- genes are shown. Arrows indicate the positions of APA sites. The depicted rat APAs are from this current dataset. Circadian rat APAs are indicated with asterisks. The 3' UTR lengths are 5,125, 5,008 and 8,004 n.t. for human, mouse, and rat, respectively. Mouse and rat sequence comparison by BLAST produced 4 segments having 91%, 83%, 86% and 82% identity for regions 1, 2, 3 and 4, depicted by blue bars.

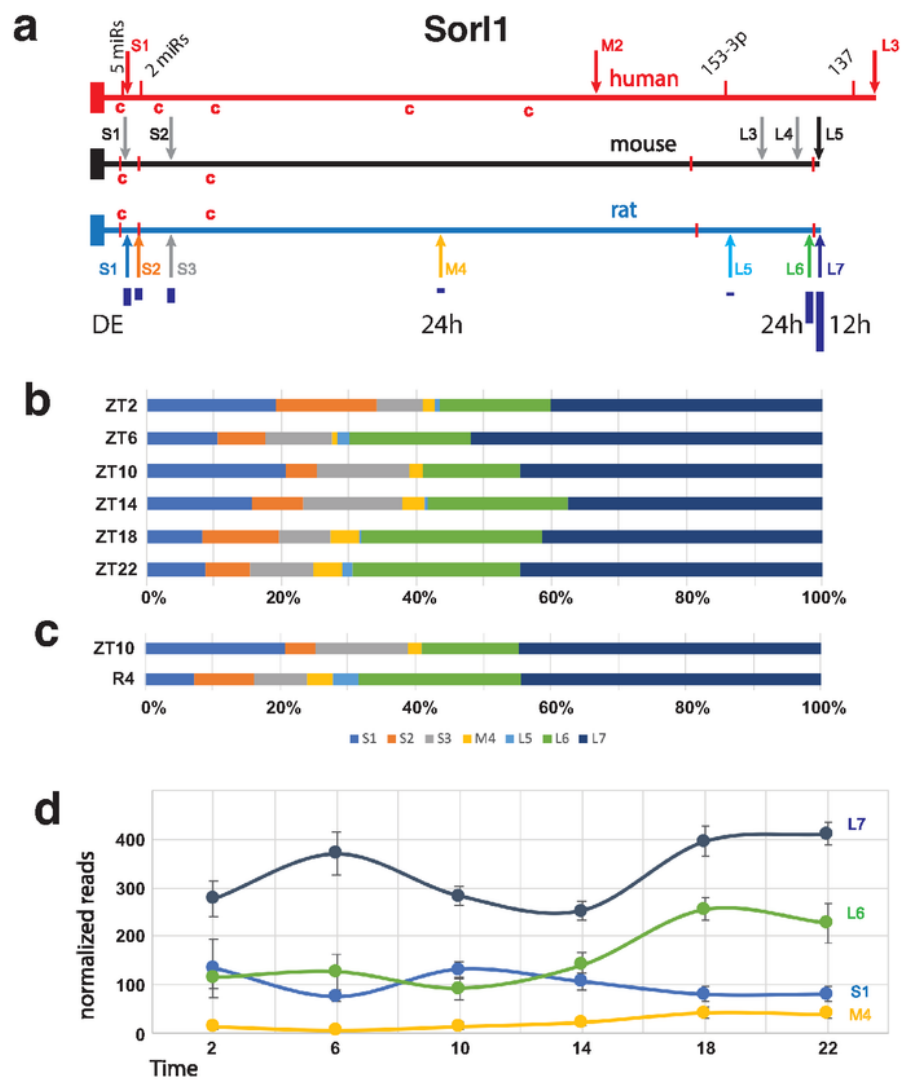


**Figure 4**

Map and APA read analyses of *Sorl1*. **(a)** Maps of the human, mouse and rat *Sorl1* gene 3' UTRs show APA sites indicated by arrows. Four highly conserved miR binding sites are marked by red bars in all three species. The first 2 are recognized by multiple miRs. The size of dark blue bars under the rat APAs depict the individual proportion compared to the total of all WTTS *Sorl1* reads. The human APAs are from established isoforms which also include different exon configurations. The first 4 mouse APAs are

suggested by ESTs, and, in the latter 3 cases, by upstream polyA signals and PolyA\_DB v3 data. Red 'c's indicate matches to the consensus CPE sites. **(b)** The proportion each *Sorl1* APA contributes to the total for the gene are plotted for each of the circadian timepoints. **(c)** The proportion each *Sorl1* APA contributes to the total for the gene are plotted for the differentially expressed samples: ZT10 and 4 hours after SD. **(d)** Graph of normalized read numbers of 4 *Sorl1* APAs that either cycle with 24 h (M4 and L6) or 12 h (L7) hours and the one differentially expressed after SD (S1).

## Supplementary Files

This is a list of supplementary files associated with this preprint. Click to download.

- [SupplFigureS1NewroseplotAPABH.QandrAmp.ai](#)
- [SupplFigureS2Homer1APAsratoronly.ai](#)
- [SupplTableS1aallPASsrawreadnumbers18.xlsx](#)
- [SupplTableS2allcircadianPASs11823.xlsx](#)
- [SupplTableS3circadianGOandPathwayforgeneswith2APAs.xlsx](#)
- [SupplTableS4CircadianGOandpathwaybyphaseusinggeneswith2APAs11723.xlsx](#)
- [SupplTableS5All12hcyclingPASs11723.xlsx](#)
- [SupplTableS6GOandPathway12hcyclingfromgeneswith2APAs.xlsx](#)
- [SupplTableS7DEPASsforZT6vsR0andZT10vsR42APAs.xlsx](#)
- [Tables.docx](#)